

$\alpha + {}^{28}\text{Si}$ and ${}^{16}\text{O}+{}^{16}\text{O}$ molecular states, and their isoscalar monopole strengths

Masaaki Kimura*

Department of Physics, Hokkaido University, Sapporo 060-0810, Japan

Nuclear Reaction Data Centre (JCPRG),

Hokkaido University, Sapporo 060-0810, Japan and

Research Center for Nuclear Physics (RCNP),

Osaka University, Ibaraki 567-0047, Japan

Yasutaka Taniguchi†

Department of Information Engineering,

National Institute of Technology (KOSEN),

Kagawa College, Mitoyo 769-1192, Japan and

Research Center for Nuclear Physics (RCNP),

Osaka University, Ibaraki 567-0047, Japan

(Dated: May 22, 2020)

Abstract

The properties of the $\alpha+{}^{28}\text{Si}$ and ${}^{16}\text{O}+{}^{16}\text{O}$ molecular states which are embedded in the excited states of ${}^{32}\text{S}$ and can have an impact on the stellar reactions, are investigated using the antisymmetrized molecular dynamics. From the analysis of the cluster spectroscopic factors, the candidates of $\alpha+{}^{28}\text{Si}$ and ${}^{16}\text{O}+{}^{16}\text{O}$ molecular states are identified close to and above the cluster threshold energies. The calculated properties of the $\alpha+{}^{28}\text{Si}$ molecular states are consistent with those reported by the $\alpha+{}^{28}\text{Si}$ resonant scattering experiments. On the other hand, the ${}^{16}\text{O}+{}^{16}\text{O}$ molecular state, which is predicted to be identical to the superdeformation of ${}^{32}\text{S}$, is inconsistent with the assignment proposed by an α inelastic scattering experiment. Our calculation suggests that the monopole transition from the ground state to the ${}^{16}\text{O}+{}^{16}\text{O}$ molecular state is rather weak and is not strongly excited by the α inelastic scattering.

* masaaki@nucl.sci.hokudai.ac.jp

† taniguchi-y@di.kagawa-nct.ac.jp

I. INTRODUCTION

The $\alpha+^{28}\text{Si}$ and $^{16}\text{O}+^{16}\text{O}$ molecular states [1–5] which is embedded in the excited states of ^{32}S are fascinating subjects in nuclear cluster physics and nuclear astrophysics. The α -induced reactions such as $^{28}\text{Si}(\alpha, \gamma)^{32}\text{S}$ and $^{28}\text{Si}(\alpha, p)^{31}\text{P}$ play an important role in the silicon burning process of the stellar evolution and nucleosynthesis [6]. The $\alpha+^{28}\text{Si}$ molecular states, if they exist at the incident energy, increase the reaction rate in order of magnitude and determine the reaction products [7–9]. In a similar manner, the $^{16}\text{O}+^{16}\text{O}$ molecular states crucially affect the oxygen burning process [10–18]. Furthermore, the $^{16}\text{O}+^{16}\text{O}$ molecular states have unique and interesting characteristics from the view point of nuclear cluster physics. Many theoretical studies [19–26] predicted that an $^{16}\text{O}+^{16}\text{O}$ molecular band should exist just below the $^{16}\text{O}+^{16}\text{O}$ threshold energy, and it must be identical to the superdeformed state of ^{32}S . Although the superdeformation of ^{32}S has not been observed, the theoretical prediction sheds a new light on the clustering of light nuclei.

Experimentally, these molecular states have been explored using the ordinary techniques such as transfer reactions [27–32] and resonant scattering [33–37]. However, as the molecular states are embedded in the continuum of ^{32}S , it is difficult to identify them from many other resonances. This difficulty prevents us from the full understanding of the molecular states and the superdeformation.

In this decade, instead of the ordinary experimental techniques, the isoscalar monopole and dipole transitions induced by α inelastic scattering are attracting a lot of research interest to overcome the above-mentioned problem. These transitions can populate the deep sub-barrier resonances and have unique selectivity for molecular states; hence, they are effective to identify the molecular states embedded in the continuum [38–41]. In particular, the method has already been successfully applied to the discussion of clustering and molecular states in many stable and unstable nuclei [42–55]. On the same line of physics, Itoh *et al.* [56] have measured the isoscalar transitions of ^{32}S , identified several excited states with enhanced transition strengths, and proposed a new band assignment for the $\alpha+^{28}\text{Si}$ and $^{16}\text{O}+^{16}\text{O}$ molecular states (and hence the superdeformed states of ^{32}S).

In this work, motivated by the new and interesting experimental data, we theoretically investigated the $\alpha+^{28}\text{Si}$ and $^{16}\text{O}+^{16}\text{O}$ molecular states, and their monopole strengths. The framework of the antisymmetrized molecular dynamics (AMD) [57–59] has already been

applied to the study of the molecular states and superdeformation of *sd-pf* nuclei [21, 60–63]. Recently it has been extended to handle the rotation effect of the deformed clusters and successfully applied to investigate the $^{12}\text{C} + ^{16}\text{O}$ molecular states at deep sub-barrier energy [64]. Following these studies, we extended our researches considering both the $\alpha + ^{28}\text{Si}$ and $^{16}\text{O} + ^{16}\text{O}$ channels in addition to the rotation effect of the deformed ^{28}Si cluster. It was found that the monopole transition has a strong selectivity to $\alpha + ^{28}\text{Si}$ molecular states, but it is insensitive to $^{16}\text{O} + ^{16}\text{O}$ molecular states. Consequently, we conclude that many of the excited states reported by Itoh *et al.* [56] should be attributed to the $\alpha + ^{28}\text{Si}$ molecular states. From the systematics of the cluster spectroscopic factors and $B(E2)$ transition strengths, we also propose the assignment of the $\alpha + ^{28}\text{Si}$ and $^{16}\text{O} + ^{16}\text{O}$ molecular bands.

This paper is organized as follows: In the next section, we explain the AMD framework and how we handle both the $\alpha + ^{28}\text{Si}$ and $^{16}\text{O} + ^{16}\text{O}$ channels, as well as the rotation effect of the deformed ^{28}Si cluster. In section III, we explain the $\alpha + ^{28}\text{Si}$ and $^{16}\text{O} + ^{16}\text{O}$ wave functions obtained by the variational calculations. We discuss the properties of the 0^+ states and their monopole strengths in comparison with the observations. We also suggest the $\alpha + ^{28}\text{Si}$ and $^{16}\text{O} + ^{16}\text{O}$ molecular band assignment. The final section summarizes this work.

II. THEORETICAL FRAMEWORK

The theoretical framework used in this paper is the same as our previous work for the $^{12}\text{C} + ^{16}\text{O}$ molecular states. The deformed-basis AMD is combined with the *d*-constraint method. The Hamiltonian is expressed as,

$$H = \sum_{i=1}^A t(i) + \sum_{i<j}^A v_{NN}(ij) + \sum_{i<j}^A v_C(ij) - t_{\text{c.m.}}, \quad (1)$$

where the Gogny D1S parameter set [65] is used for the effective nucleon-nucleon interaction v_{NN} and the Coulomb interaction v_C is approximated by a sum of seven Gaussians. The center-of-mass kinetic energy $t_{\text{c.m.}}$ is properly removed from the Hamiltonian without any approximation. This Hamiltonian reasonably describes the threshold energies of interest without any adjustment. The $\alpha + ^{28}\text{Si}$ and $^{16}\text{O} + ^{16}\text{O}$ threshold energies measured from the ^{32}S ground state are calculated as 7.56 and 16.25 MeV, respectively, which are compared with the experimental data 6.95 and 16.54 MeV.

The variational wave function of the deformed-basis AMD is a parity-projected Slater determinant of the single-particle wave packets [66],

$$\begin{aligned}\Phi &= \mathcal{A} \{ \varphi_1, \dots, \varphi_A \}, \\ \varphi_i &= \prod_{\sigma=x,y,z} \left(\frac{2\nu_\sigma}{\pi} \right)^{1/4} \exp \{ -\nu_\sigma (r_\sigma - Z_{i\sigma})^2 \} \\ &\quad \times (\alpha_i |\xi_\uparrow\rangle + \beta_i |\xi_\downarrow\rangle) \times (|p\rangle \text{ or } |n\rangle),\end{aligned}\tag{2}$$

$$\tag{3}$$

where each of the φ_i has the deformed Gaussian form and has the parameters: the centroid of the Gaussian \mathbf{Z}_i , size parameter $\boldsymbol{\nu}$ and spin direction α_i and β_i . The isospin part is fixed to either of proton or neutron. The size parameter $\boldsymbol{\nu}$ is a real-valued vector, but the other parameters are complex-valued. They are determined by the energy variation with two different constraints. The first one is the constraint on the quadrupole deformation parameter β , which we call the β -constraint. It is noted that the β -constraint was already used to study the superdeformation of ^{32}S and the $^{16}\text{O}+^{16}\text{O}$ molecular states within the AMD framework [21]. The second constraint is imposed on the inter-cluster distance between the α and ^{28}Si clusters, and between two ^{16}O clusters, which we call the d -constraint [67]. We classify the centroids of the wave packets into two groups corresponding to the cluster configurations, and define an approximate inter-cluster distance d as the distance between the center-of-masses of two groups. For example, d for $\alpha+^{28}\text{Si}$ configuration is defined as,

$$d = \left| \frac{1}{4} \sum_{i \in \alpha} \text{Re} \mathbf{Z}_i - \frac{1}{28} \sum_{i \in ^{28}\text{Si}} \text{Re} \mathbf{Z}_i \right|.\tag{4}$$

The value of d is constrained from 2 fm to 8 fm with the interval of 0.5 fm. It is emphasized that the d -constraint is essential for describing the $\alpha+^{28}\text{Si}$ molecular states, because the β -constraint yields only the mean-field and $^{16}\text{O}+^{16}\text{O}$ molecular states. Furthermore, it can handle the cluster polarization effect and the rotation effect of the deformed clusters in a natural manner.

From the energy variation with the constraints, we obtain the wave functions which have the minimum energies for each given value of β or d . After the energy variation, the wave functions are projected to the eigenstates of the angular momentum, and superposed to diagonalize the Hamiltonian (generator coordinate method; GCM).

$$\Psi_{M\alpha}^{J\pi} = \sum_{iK} b_{iK\alpha} P_{MK}^J \Phi^\pi(\beta_i) + \sum_{iK} d_{iK\alpha} P_{MK}^J \Phi^\pi(d_i),\tag{5}$$

where P_{MK}^J denotes the angular momentum projector, $\Phi^\pi(\beta_i)$ and $\Phi^\pi(d_i)$ are the wave functions obtained by the β - and d -constraints, respectively. The coefficients of the superposition b_{iK} and d_{iK} are determined by solving the Hill-Wheeler equation [68].

As a measure for the $\alpha+^{28}\text{Si}$ and $^{16}\text{O}+^{16}\text{O}$ clustering, we calculate the reduced width amplitude (RWA), which is the probability amplitude to find the clusters at the inter-cluster distance a . It is defined as the overlap between the reference cluster wave function and the GCM wave function given by Eq. (5),

$$y_\ell(a) = \sqrt{\frac{32!}{C_1!C_2!}} \left\langle \frac{\delta(r-a)}{r^2} [\Phi_{C_1} \Phi_{C_2} Y_\ell(\hat{r})]_M^J \middle| \Psi_{M\alpha}^{J\pi} \right\rangle, \quad (6)$$

where $C_{1,2}$ and Φ_{C_1,C_2} denote the masses and wave functions of clusters, respectively: $C_1 = 4$ and $C_2 = 28$ for the $\alpha+^{28}\text{Si}$ configurations, and $C_1 = C_2 = 16$ for the $^{16}\text{O}+^{16}\text{O}$ configurations. The reference wave function (bra state) describes the system in which two clusters with the masses of C_1 and C_2 are mutually orbiting with the angular momentum ℓ and the inter-cluster distance a . Here, the wave functions of the α and ^{16}O clusters are assumed to be the harmonic oscillator wave functions with the doubly closed shell structure, which reproduce the observed charge radii. The wave function of the ^{28}Si cluster is approximated using a single AMD wave function projected to either of $J^\pi = 0^+$ or 2^+ states. The Eq. (6) was calculated using the Laplace expansion method [69] for the $\alpha+^{28}\text{Si}$ channel and using the projection method to the Brink wave function [70, 71] for the $^{16}\text{O}+^{16}\text{O}$ channel. The cluster spectroscopic factors in these channels are calculated by the squared integral of y_ℓ .

$$S_\ell = \int_0^\infty da a^2 |y_\ell(a)|^2, \quad (7)$$

which is enhanced for the developed cluster states, and is used to identify the molecular states.

In this work, we focus on the isoscalar monopole ($IS0$) transition strength which has been regarded and utilized as a novel probe for the molecular states in stable and unstable nuclei. The transition operator is defined as follows,

$$\mathcal{M}^{IS0} = \sum_{i=1}^A r_i'^2. \quad (8)$$

Note that the single-particle coordinate \mathbf{r}'_i is measured from the center-of-mass $\mathbf{r}_{\text{c.m.}}$, *i.e.* $\mathbf{r}'_i \equiv \mathbf{r}_i - \mathbf{r}_{\text{c.m.}}$; hence, our calculation is free from the spurious center-of-mass contributions.

The reduced transition matrix from the ground state to the excited 0^+ state is calculated as

$$M(ISO; 0_1^+ \rightarrow 0_{\text{ex.}}^+) = \langle \Psi(0_{\text{ex.}}^+) | \mathcal{M}^{ISO} | \Psi(0_{\text{g.s.}}^+) \rangle, \quad (9)$$

where $\Psi(0_{\text{g.s.}}^+)$ and $\Psi(0_{\text{ex.}}^+)$ are the wave functions of the ground and excited 0^+ states, respectively.

III. RESULTS AND DISCUSSIONS

A. Molecular configurations obtained by the variational calculations

Figure 1 (a) shows the energy curves of the positive-parity states obtained by the β -constraint. It has two minima at $\beta = 0.32$ and 0.72 after the angular momentum projection, which correspond to the ground state and superdeformed state, respectively. Their intrinsic density distributions shown in Fig. 2 (b) and (d) appear considerably different and impress the exotic shape of the superdeformed minimum (panel (d)) which is extremely deformed with a neck and two-centered. Similar density distributions of the superdeformed state have also been reported by many other theoretical studies [21–26, 72–74].

The energy curves for the $\alpha+^{28}\text{Si}$ and $^{16}\text{O}+^{16}\text{O}$ molecular configurations obtained by the d -constraint are shown in Fig. 1 (b). We have obtained two different $\alpha+^{28}\text{Si}$ molecular configurations which have different orientations of the deformed ^{28}Si cluster. We call them S- and L-type configurations in the following. In the S-type configuration denoted by (S), the symmetry axis of the oblate deformed ^{28}Si cluster is parallel to the x -axis on which the center-of-mass of α and ^{28}Si clusters are placed (see Fig. 2 (f) and (g)). On the contrary, in the L-type configuration (L), the symmetry axis of ^{28}Si is perpendicular to the x -axis (see Fig. 2 (h) and (i)). By mixing both the S- and L-type configurations, we can handle the rotation effect of the deformed ^{28}Si cluster within the AMD framework. It is also noted that these two configurations have different single-particle structure at a small inter-cluster distance. The S-type configuration approaches the ground state configuration ($0\hbar\omega$) at a short inter-cluster distance; hence, its energy ($E = -267.0$ MeV at $d = 2.5$ fm) is close to that of the ground state minimum ($E = -268.9$ MeV at $\beta = 0.25$) as shown in Fig. 1. It is important to note that the squared overlaps of the wave functions between the ground state and the S-type $\alpha+^{28}\text{Si}$ configurations are non-negligible after the parity and angular-momentum projection to $J^\pi = 0^+$, although they appear quite different at a glance.

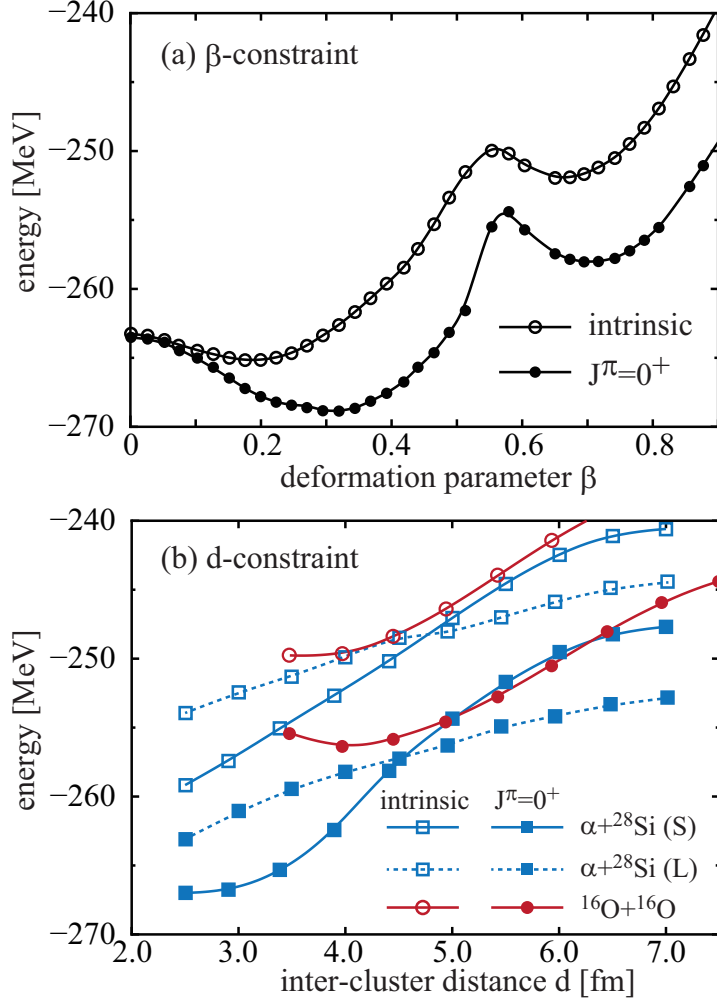


FIG. 1. (color online) Energy curves of the positive-parity states before (intrinsic) and after the angular momentum projection to $J^\pi = 0^+$. (a) The energy curves obtained by the constraint on the quadrupole deformation parameter β . (b) The energy curves of the $\alpha+^{28}\text{Si}$ and $^{16}\text{O}+^{16}\text{O}$ molecular configurations.

Indeed, the overlap between the wave functions shown in Figs. 2 (b) and (f) is as large as 0.45. On the contrary, the L-type configuration approaches a $4\hbar\omega$ excited configuration at a small distance. Consequently, the L-type configurations are orthogonal to the ground state configuration and their energies are relatively higher than the S-type configurations. It is noted that these different asymptotics of the molecular configurations play a crucial role for the isoscalar monopole transitions.

The $^{16}\text{O}+^{16}\text{O}$ configuration is almost identical to the superdeformed state (a $4\hbar\omega$ configuration) at the energy minimum ($d = 3.5$ fm), and its energy (-257.6 MeV) is very close

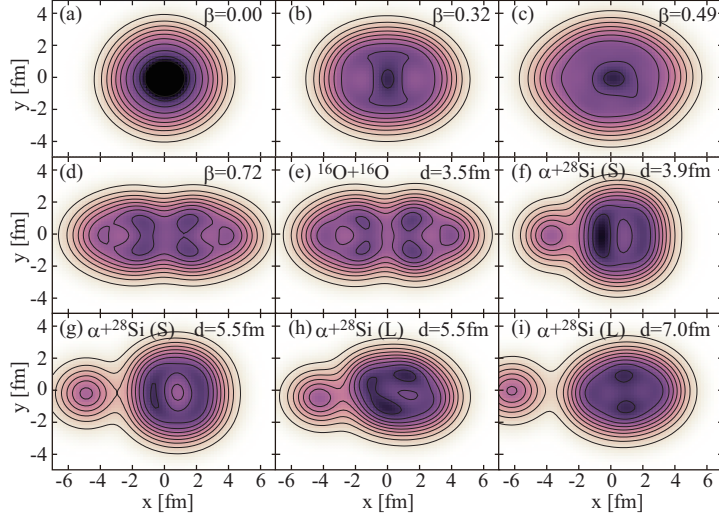


FIG. 2. (color online) (a)-(d): The intrinsic densities obtained by the β -constraint. The panels (b) and (d) correspond to the ground and superdeformed minima on the energy surface, respectively. (e)-(i): The intrinsic densities obtained by the d -constraint. The panel (e) shows the intrinsic density of the $^{16}\text{O}+^{16}\text{O}$ configuration at the energy minimum. The panels (f) and (g) are the S-type $\alpha+^{28}\text{Si}$ configurations in which the symmetry axis of the ^{28}Si cluster is parallel to the x -axis, while the panels (h) and (i) are the L-type configurations in which the shortest axis is perpendicular to the x -axis.

to that of the superdeformed minimum (-258.0 MeV). It is impressive that their density distributions are significantly similar to each other (Fig. 2 (d) and (e)), and the squared overlap of their wave functions is as large as 0.92 which indicates that they are actually identical. This is the reason why many theoretical studies [20–26, 72] discuss the similarity of the superdeformation of ^{32}S and the $^{16}\text{O}+^{16}\text{O}$ molecular states. However, despite the consistent and convincing discussions by many theories, experimental information about the superdeformation of ^{32}S had been rather limited [32, 75]. Recently, Itoh *et al.* [56] provided a new report by investigating the isoscalar monopole transition strengths of ^{32}S . In particular, based on the observed strong monopole transitions, they proposed a new assignment of the $^{16}\text{O}+^{16}\text{O}$ molecular states, and hence the superdeformed states. We will verify their assignment in the following sections.

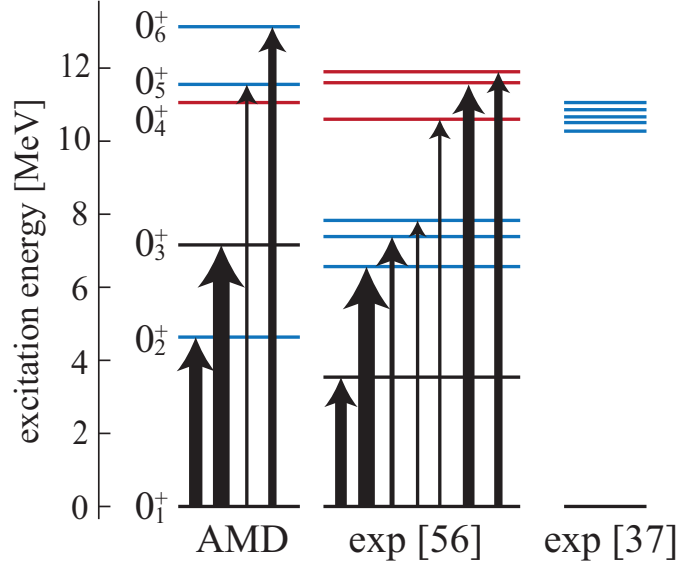


FIG. 3. (color online) The calculated and observed [37, 56] candidates of the $\alpha+^{28}\text{Si}$ (blue lines) and $^{16}\text{O}+^{16}\text{O}$ (red lines) molecular states with $J^\pi = 0^+$. The widths of the arrows are proportional to the isoscalar monopole transition matrix.

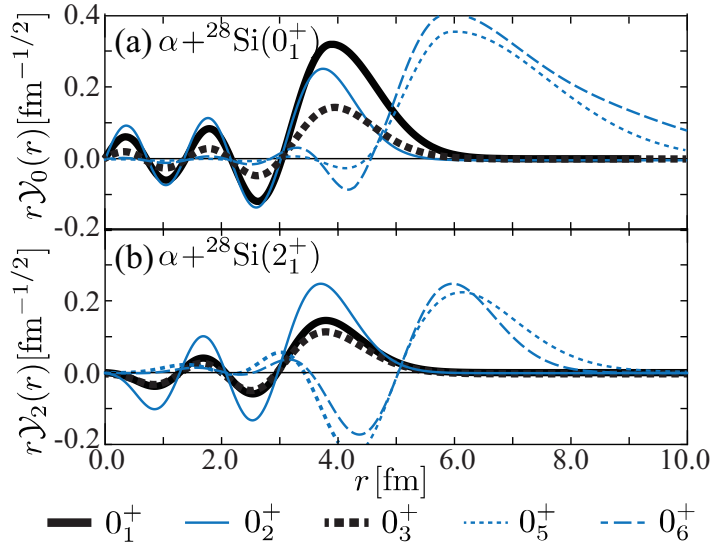


FIG. 4. (color online) The reduced width amplitudes in the $\alpha+^{28}\text{Si}(0_1^+)$ and $\alpha+^{28}\text{Si}(2_1^+)$ channels calculated for the 0_1^+ , 0_2^+ , 0_3^+ , 0_5^+ and 0_6^+ states, respectively.

TABLE I. The calculated excitation energies in MeV, isoscalar monopole transition matrices in fm^2 and cluster spectroscopic factors of the 0^+ states. $S_{\alpha\ell=0}$, $S_{\alpha\ell=2}$ and S_O denote the spectroscopic factors in the $\alpha+^{28}\text{Si}(0_1^+)$, $\alpha+^{28}\text{Si}(2_1^+)$ and $^{16}\text{O}+^{16}\text{O}$ channels, respectively. The observed excitation energies and the isoscalar monopole matrices [56] are also listed.

	AMD					exp.	
	E_x	$M(ISO)$	$S_{\alpha,\ell=0}$	$S_{\alpha,\ell=2}$	S_O	E_x	$M(ISO)$
0_1^+	0.0		0.09	0.04	0.00	0.0	
0_2^+	4.6	5.7	0.05	0.06	0.00	3.78	4.0
0_3^+	7.0	6.5	0.02	0.01	0.02	6.59	6.3
						7.65	3.8
						7.95	2.7
0_4^+	11.0	0.0	0.02	0.01	0.32		
0_5^+	11.6	2.8	0.29	0.14	0.00	11.49	3.3
0_6^+	13.1	4.8	0.34	0.12	0.02	11.62	5.4
						11.90	4.3

B. Molecular states and their monopole strengths

In this section, we focus on the $J^\pi = 0^+$ states, and discuss their molecular structure, monopole transition strengths and experimental candidates. However, before the discussion of the present results, it may be useful to summarize the experimental information about the $\alpha+^{28}\text{Si}$ and $^{16}\text{O}+^{16}\text{O}$ molecular states. Many resonances which are the candidates of the $\alpha+^{28}\text{Si}$ molecular states have been reported above the $\alpha+^{28}\text{Si}$ threshold energy by the resonant scattering experiments [34–37]. In particular, Lönnroth *et al.* [37] comprehensively summarized the observed resonances covering broad energy region, and proposed an $\alpha+^{28}\text{Si}$ molecular band. The candidates of the 0^+ resonances they proposed are fragmented into many states in between 10.25 and 11.05 MeV as shown in Fig. 3. They all have the α decay widths ranging from a few keV to a few tens keV, and many of them coincide with the resonances observed in other experiments [34–36]. The α transfer reaction [27–31] is another useful probe for the $\alpha+^{28}\text{Si}$ molecular states, especially for the states below the decay threshold. Peng. *et al.* [29, 30] and Tanabe *et al.* [31] reported the α spectroscopic

factor of the 0_2^+ states by means of the ($^{16}\text{O}, ^{12}\text{C}$) and ($^6\text{Li}, d$) reactions, respectively. They concluded that the α spectroscopic factor of the 0_2^+ state is approximately 0.50-0.75 relative to that of the ground state (it varies, depending on the incident energy). Tanabe *et al.* also reported that several states at 10 to 11 MeV are strongly populated by the ($^6\text{Li}, d$) reaction, and hence, suggested as the candidates of the $\alpha+^{28}\text{Si}$ molecular states. Although the spin-parity assignment was not discussed, it is important to note that the energies of these states are very close to the 0^+ resonances reported by Lönnroth *et al.* [37].

The isoscalar monopole strength is a novel probe for the molecular states, and has a unique selectivity. Itoh *et al.* [56] measured the isoscalar monopole transitions of ^{32}S by the α inelastic scattering, and reported several states as the candidates of the molecular states. In addition to the 0_2^+ state, they found that six excited states have the enhanced monopole strength as listed in Table I. They are classified into two groups; three states at 6 to 8 MeV and the other three at 10 to 12 MeV. As summarized in Fig. 3, the former group was proposed as the $\alpha+^{28}\text{Si}$ molecular states, and the latter as the $^{16}\text{O}+^{16}\text{O}$ molecular states. Furthermore, the latter group, the states at 10 to 12 MeV, is also proposed as the superdeformed states, because the $^{16}\text{O}+^{16}\text{O}$ molecular state and the superdeformation should be identical. To summarize the experimental data, the 0^+ resonances at 10 to 12 MeV are observed in many experiments. They are assigned as the $\alpha+^{28}\text{Si}$ molecular states in Refs. [31, 34–37], but are assigned as the $^{16}\text{O}+^{16}\text{O}$ molecular states in Ref. [56]. Itoh *et al.* also reported another group of the states at 6 to 8 MeV and assigned them as the $\alpha+^{28}\text{Si}$ molecular states.

Now, we discuss the present numerical results in comparison with the above-mentioned experimental data. The calculated ground state is predominated by the mean-field configuration shown in Fig. 2 (b). The squared overlap between the ground state and this configuration is 0.92. It is noted that the ground state also has a large overlap with the S-type $\alpha+^{28}\text{Si}$ molecular configurations with small inter-cluster distances. The overlap between the ground state and the $\alpha+^{28}\text{Si}$ configuration shown in Fig. 2 (f) is as large as 0.46 and the calculated spectroscopic factors of the ground state are $S_\alpha = 0.09$ and 0.04 in the $\alpha+^{28}\text{Si}(0_1^+)$ and $\alpha+^{28}\text{Si}(2_1^+)$ channels, respectively. This indicates that the α cluster correlation exists even in the ground state. In fact, the calculated RWA of the ground state (Fig. 4) has a peak at 3 to 4 fm showing the α cluster formation at the nuclear surface. These results qualitatively agree with the observed large cross section of $^{32}\text{S}(p, p\alpha)^{28}\text{Si}$ [76] which

is sensitive to the α cluster formation at the surface of the ground state [77–81]. On the other hand, the ground state has no overlap with the L-type $\alpha+^{28}\text{Si}$ and $^{16}\text{O}+^{16}\text{O}$ configurations as they asymptotically approach the $4\hbar\omega$ excited configurations at zero inter-cluster distance, and are almost orthogonal to the ground state.

The 0_2^+ state largely consists of almost the spherical configuration shown in Fig. 2 (a), and their squared overlap is 0.67. In addition, it also has a non-negligible overlap with the S-type $\alpha+^{28}\text{Si}$ molecular configuration. The overlap between the 0_2^+ state and the $\alpha+^{28}\text{Si}$ configuration shown in Fig. 2 (f) is 0.22, which indicates the non-negligible α cluster correlation in this state. The calculated RWA and α spectroscopic factors are not as large as those of the ground state, and the ratio of S_α to the ground state is $S_{\alpha,\ell=0}(0_2^+)/S_{\alpha,\ell=2}(0_1^+) = 0.56$. This reduction of the S_α relative to the ground state reasonably agrees with the observed values which is in between 0.51 and 0.75 [29–31]. It must be emphasized that the α cluster correlations in the ground and 0_2^+ states are the origin of the large monopole transition strength (5.7 fm^2) between these states. In fact, if we exclude the $\alpha+^{28}\text{Si}$ molecular configurations from the GCM calculation, the spectroscopic factors of the ground and 0_2^+ states are reduced to 0.05 and 0.02 in the $\alpha+^{28}\text{Si}(0_1^+)$ channel, and the monopole transition matrix is reduced to 2.32 fm^2 which is smaller than the observed value, 4.0 fm^2 .

The 0_3^+ state has the largest overlap with the configuration shown in Fig. 2 (c) which amounts to 0.36. This state has similar magnitude of the overlap with many other configurations on the β -constraint energy surface shown in Fig. 1 (a), but it scarcely overlaps with the molecular configurations. Therefore, its RWA and spectroscopic factors are small, and we conclude that the 0_3^+ state is a β -vibration state. This interpretation explains the large monopole strength of this state, as it is well known that the β -vibration also enhances the monopole transition strengths [82]. Itoh *et al.* [56] observed three 0^+ states (6.59, 7.65 and 7.95 MeV states) with the enhanced monopole strengths in this energy region, and 6.59 MeV state plausibly coincides with the calculated 0_3^+ state. However, neither of our calculation nor other experiments reported additional 0^+ states in between 6 to 8 MeV [83]. Therefore, more detailed study is needed to confirm the 7.65 and 7.95 MeV states.

The 0_4^+ state is the superdeformed state which was already discussed in the previous AMD study [21]. It has the large squared overlap (0.95) with the configuration shown in Fig. 2 (d). In addition, it also has large overlap with the $^{16}\text{O}+^{16}\text{O}$ configuration shown in Fig. 2 (e), that amounts to 0.92. Hence, the superdeformed state of ^{32}S is regarded as an $^{16}\text{O}+^{16}\text{O}$ molecular

state; *i.e.* it has a duality of the superdeformation and clustering. From the observed strong monopole transitions, Itoh *et al.* proposed the 10.49, 11.62 and 11.90 MeV states as the superdeformed states. However, in contrast to their assignment, the present calculation shows that the monopole transition to the superdeformed state is negligible. This result clearly reflects the nature of the monopole transition. As explained by Yamada *et al.* [40], the monopole transition excites the molecular configurations which are contained in the ground state. In other words, the molecular configurations orthogonal to the ground state at zero inter-cluster distance are not populated by the monopole transition. Because the $^{16}\text{O}+^{16}\text{O}$ configuration is orthogonal to the ground state, the monopole transition from the ground state to the $^{16}\text{O}+^{16}\text{O}$ molecular state is strictly forbidden. Therefore, the present result does not support the assignment of the $^{16}\text{O}+^{16}\text{O}$ molecular state and the superdeformed state observed in the α inelastic scattering experiment.

The 0_5^+ and 0_6^+ states are the highly excited $\alpha+^{28}\text{Si}$ molecular states which overlap with both the S- and L-type $\alpha+^{28}\text{Si}$ configurations shown in Figs. 2 (f)-(i). As seen in Table I, these states are predominated by the $\alpha+^{28}\text{Si}(0_1^+)$ channel, while the ground state and 0_2^+ states are the mixture of the $\alpha+^{28}\text{Si}(0_1^+)$ and $\alpha+^{28}\text{Si}(2_1^+)$ channels. This is because of the weak interaction between the clusters in the 0_5^+ and 0_6^+ states, which de-excites the ^{28}Si cluster to its ground state (weak cluster polarization). Note that the RWA of the 0_5^+ and 0_6^+ states have a peak at approximately 6 fm, which indicates the large inter-cluster distance and enhanced clustering. Owing to this pronounced $\alpha+^{28}\text{Si}$ molecular structure, these states have large monopole transition strengths, and they may correspond to any of the 10.49, 11.62 and 11.90 MeV states observed by Itoh *et al.* Interestingly, the $\alpha+^{28}\text{Si}$ molecular states observed by Lönnroth *et al.* are located at the same energy region, and we consider that they are the same $\alpha+^{28}\text{Si}$ molecular states.

Thus, the present calculation has revealed the characteristics of the excited 0^+ states. The monopole transition from the ground state has a selectivity, because the ground state is a mixture of the deformed mean-field and $\alpha+^{28}\text{Si}$ molecular structure. The β -vibration state and $\alpha+^{28}\text{Si}$ molecular states are strongly excited, but the $^{16}\text{O}+^{16}\text{O}$ molecular state (and hence the superdeformed state) is not. We conclude that many of the states with enhanced monopole strengths observed below 12 MeV should be attributed to the $\alpha+^{28}\text{Si}$ molecular states.

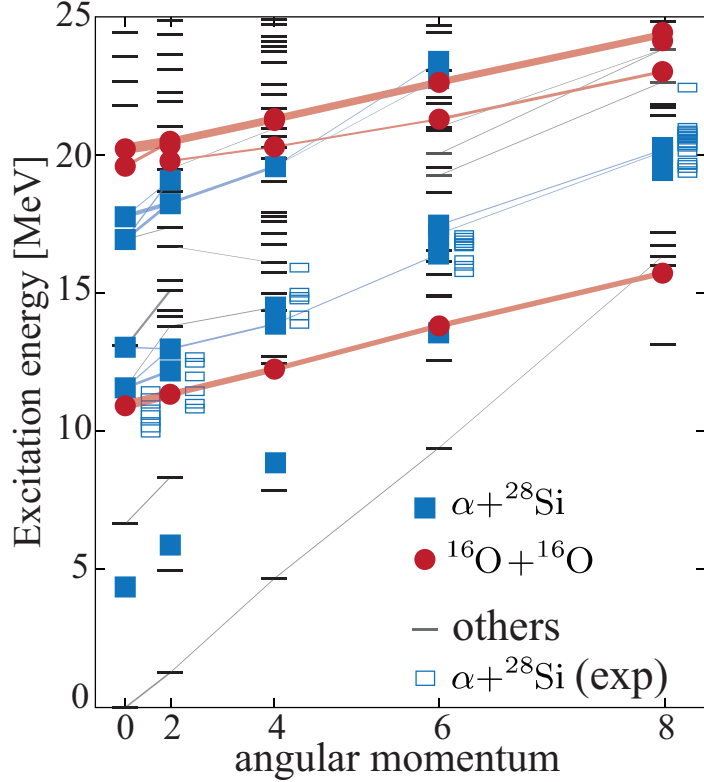


FIG. 5. (color online) The calculated molecular bands up to $J^\pi = 8^+$ states. The filled squares and circles show the $\alpha+^{28}\text{Si}$ and $^{16}\text{O}+^{16}\text{O}$ molecular states, respectively. The open squares show the observed candidates of the $\alpha+^{28}\text{Si}$ molecular band [37]. The $B(E2 \uparrow)$ transitions stronger than $150 e^2\text{fm}^4$ are shown by the connecting lines whose widths are proportional to the magnitude of the transition matrices.

C. Assignment of the rotational bands

Figure 5 shows our assignment of the $\alpha+^{28}\text{Si}$ and $^{16}\text{O}+^{16}\text{O}$ molecular bands from the present calculation. The assignment is based on the calculated spectroscopic factors. That is, if the spectroscopic factors in the $^{16}\text{O}+^{16}\text{O}$ channel or if the sum of the spectroscopic factors in the $\alpha+^{28}\text{Si}(0_1^+)$ and $\alpha+^{28}\text{Si}(2_2^+)$ channels is larger than 0.10, we have assigned the state as the molecular state. The figure also shows the $B(E2 \uparrow)$ strengths larger than $150 e^2\text{fm}^4$, which confirms that most of the molecular states are connected by the strong $B(E2)$ transitions due to their strong quadrupole deformation.

The assignment of the $^{16}\text{O}+^{16}\text{O}$ band is essentially same with that proposed in the previous AMD study and rather unique as it does not strongly fragment into many states. The

lowest $^{16}\text{O}+^{16}\text{O}$ band is built on the 0_4^+ state at 11.0 MeV, and as already discussed in Ref. [21], it is identical to the superdeformed band with huge moment-of-inertia as large as $\hbar^2/(2\mathcal{I}) = 68$ keV. Another $^{16}\text{O}+^{16}\text{O}$ molecular band, in which the relative motion between ^{16}O clusters is excited, exists at approximately $E_x = 20$ MeV, and the member states of this band with $J \geq 2$ are fragmented into two or three states.

The assignment of the $\alpha+^{28}\text{Si}$ band is not as unique as the $^{16}\text{O}+^{16}\text{O}$ case since the member states are fragmented into many states due to the strong coupling of the $\alpha+^{28}\text{Si}(0_1^+)$ and $\alpha+^{28}\text{Si}(2_2^+)$ channels, as well as the coupling with the non-cluster configurations. There are many states which have small but non-negligible spectroscopic factors in the $\alpha+^{28}\text{Si}$ channels. For example, the states which have the spectroscopic factors larger than 0.05 are almost twice as many as those shown in Fig. 5. This result is consistent with the observation by Lönnroth *et al.* who reported many excited states which have small fraction of the $\alpha+^{28}\text{Si}$ spectroscopic factors. However, for the sake of clarity and simplicity, here, we discuss the states with sufficiently large spectroscopic factors (larger than 0.10). We suggest an $\alpha+^{28}\text{Si}$ band built on the 0_5^+ and 0_6^+ states. Although the member states are considerably fragmented, it can be confirmed that many states are connected by the strong $B(E2)$ transitions. We consider that this band corresponds to the $\alpha+^{28}\text{Si}$ band reported by Lönnroth *et al.* as the energies of the member states plausibly agree with their observation. We also comment that the other band, in which the relative motion of the clusters is excited, may be built on the 0^+ states approximately at 17 MeV. We can see the candidates of the band member states up to the $J^\pi = 6^+$, although the fragmentation is rather strong. Experimentally, several candidates of the $\alpha+^{28}\text{Si}$ states have been reported above 15 MeV without firm spin-parity assignment [84, 85], and the present results may explain these observations.

IV. SUMMARY

We have investigated the properties of the $\alpha+^{28}\text{Si}$ and $^{16}\text{O}+^{16}\text{O}$ molecular states in the ^{32}S excited states. An extended framework of AMD has been applied for handling both of the $\alpha+^{28}\text{Si}$ and $^{16}\text{O}+^{16}\text{O}$ channels in addition to the rotation effect of the deformed ^{28}Si cluster. It was found that the isoscalar monopole transition has the strong selectivity to the molecular states: It strongly excites the $\alpha+^{28}\text{Si}$ molecular states, but is inactive to the

$^{16}\text{O}+^{16}\text{O}$ molecular states. This selectivity originates in the different asymptotic behavior of the molecular configurations at zero inter-cluster distance. We found that the assignment of the $\alpha+^{28}\text{Si}$ molecular states proposed by Lönnroth *et al.* reasonably agrees with the present calculation, while the $^{16}\text{O}+^{16}\text{O}$ molecular state or the superdeformed state proposed by Itoh *et al.* does not, as the monopole transition strengths of the $^{16}\text{O}+^{16}\text{O}$ molecular states are rather weak and is not excited strongly by the α inelastic scattering.

ACKNOWLEDGMENTS

This work was supported by a grant for the RCNP joint research project, the collaborative research program 2020 at Hokkaido University, and JSPS KAKENHI Grant No. 19K03859.

-
- [1] D. Baye and G. Reidemeister, Nuclear Physics, Section A **258**, 157 (1976).
 - [2] T. Ando, K. Ikeda, and A. Tohsaki-Suzuki, Progress of Theoretical Physics **64**, 1608 (1980).
 - [3] D. Baye and P. Descouvemont, Nuclear Physics, Section A **419**, 397 (1984).
 - [4] K. Langanke, R. Stademann, and D. Frekers, Physical Review C **29**, 40 (1984).
 - [5] Y. Kondo, B. A. Robson, and R. Smith, Physics Letters B **227**, 310 (1989).
 - [6] D. Bodansky, D. D. Clayton, and W. A. Fowler, Physical Review Letters **20**, 161 (1968).
 - [7] P. J. Smulders, Physica **30**, 1197 (1964).
 - [8] J. W. Toevs, Nuclear Physics, Section A **172**, 589 (1971).
 - [9] D. W. Rogers, W. R. Dixon, and R. S. Storey, Nuclear Physics, Section A **281**, 345 (1977).
 - [10] H. Spinka and H. Winkler, Nuclear Physics, Section A **233**, 456 (1974).
 - [11] D. G. Kovar, D. F. Geesaman, T. H. Braid, Y. Eisen, W. Henning, T. R. Ophel, M. Paul, K. E. Rehm, S. J. Sanders, P. Sperr, J. P. Schiffer, S. L. Tabor, S. Vigdor, B. Zeidman, and F. W. Prosser, Physical Review C **20**, 1305 (1979).
 - [12] G. Hulke, C. Rolfs, and H. P. Trautvetter, Zeitschrift für Physik A Atoms and Nuclei **297**, 161 (1980).
 - [13] S. C. Wu and C. A. Barnes, Nuclear Physics, Section A **422**, 373 (1984).
 - [14] J. Thomas, Y. T. Chen, S. Hinds, D. Meredith, and M. Olson, Physical Review C **33**, 1679 (1986).

- [15] T. A. Weaver and S. E. Woosley, *Physics Reports* **227**, 65 (1993).
- [16] M. F. El Eid, B. S. Meyer, and L. The, *The Astrophysical Journal* **611**, 452 (2004), arXiv:0407459 [astro-ph].
- [17] A. Diaz-Torres, L. R. Gasques, and M. Wiescher, *Physics Letters, Section B: Nuclear, Elementary Particle and High-Energy Physics* **652**, 255 (2007).
- [18] L. R. Gasques, E. F. Brown, A. Chieffi, C. L. Jiang, M. Limongi, C. Rolfs, M. Wiescher, and D. G. Yakovlev, *Physical Review C - Nuclear Physics* **76**, 035802 (2007).
- [19] M. Freer, R. R. Betts, and A. H. Wuosmaa, *Nuclear Physics, Section A* **587**, 36 (1995).
- [20] S. Ohkubo and K. Yamashita, *Physical Review C - Nuclear Physics* **66**, 4 (2002).
- [21] M. Kimura and H. Horiuchi, *Physical Review C* **69**, 051304 (2004).
- [22] J. A. Maruhn, M. Kimura, S. Schramm, P.-G. G. Reinhard, H. Horiuchi, and A. Tohsaki, *Physical Review C* **74**, 044311 (2006).
- [23] T. Ichikawa, Y. Kanada-En'yo, P. Möller, Y. Kanada-En'yo, and P. Möller, *Physical Review C* **83**, 054319 (2011).
- [24] J.-P. P. Ebran, E. Khan, T. Nikšić, and D. Vretenar, *Physical Review C* **90**, 054329 (2014), arXiv:1406.2473.
- [25] D. Ray and A. V. Afanasjev, *Physical Review C* **94**, 014310 (2016).
- [26] J.-P. Ebran, E. Khan, T. Nikšić, and D. Vretenar, *Journal of Physics G: Nuclear and Particle Physics* **44**, 103001 (2017).
- [27] J. V. Maher, K. A. Erb, G. H. Wedberg, J. L. Ricci, and R. W. Miller, *Physical Review Letters* **29**, 291 (1972).
- [28] R. A. Lindgren, J. P. Trentelman, N. Anantaraman, H. E. Gove, and F. C. Jundt, *Physics Letters B* **49**, 263 (1974).
- [29] J. C. Peng, J. V. Maher, M. S. Chiou, W. J. Jordan, F. C. Wang, and M. W. Wu, *Physics Letters B* **80**, 35 (1978).
- [30] G. P. Berg, M. A. Fernandes, K. Nagatani, J. C. Peng, B. Berthier, J. P. Fouan, J. Gastebois, J. P. Le Fèvre, and M. C. Lemaire, *Physical Review C* **19**, 62 (1979).
- [31] T. Tanabe, M. Yasue, K. Sato, K. Ogino, Y. Kadota, Y. Taniguchi, K. Obori, K. Makino, and M. Tochi, *Physical Review C* **24**, 2556 (1981).
- [32] K. Morita, S. Kubono, M. H. Tanaka, H. Utsunomiya, M. Sugitani, S. Kato, J. Schimizu, T. Tachikawa, and N. Takahashi, *Physical Review Letters* **55**, 185 (1985).

- [33] M. Gai, E. C. Schloemer, J. E. Freedman, A. C. Hayes, S. K. Korotky, J. M. Manoyan, B. Shivakumar, S. M. Sterbenz, H. Voit, S. J. Willett, and D. A. Bromley, *Physical Review Letters* **47**, 1878 (1981).
- [34] P. Manngård, *Zeitschrift für Physik A: Hadrons and Nuclei* **349**, 335 (1994).
- [35] K. M. Källman, V. Z. Goldberg, T. Lönnroth, P. Manngård, A. E. Pakhomov, and V. V. Pankratov, *Nuclear Inst. and Methods in Physics Research, A* **338**, 413 (1994).
- [36] K.-M. Källman, M. Brenner, V. Goldberg, T. Lönnroth, P. Manngård, A. Pakhomov, and V. Pankratov, *The European Physical Journal A - Hadrons and Nuclei* 2003 16:2 **16**, 159 (2003).
- [37] T. Lönnroth, M. Norrby, V. Z. Goldberg, G. V. Rogachev, M. S. Golovkov, K. M. Källman, M. Lattuada, S. V. Perov, S. Romano, B. B. Skorodumov, G. P. Tiourin, W. H. Trzaska, A. Tumino, and A. N. Vorontsov, *The European Physical Journal A* 2010 46:1 **46**, 5 (2010).
- [38] T. Kawabata, H. Akimune, H. Fujita, Y. Fujita, M. Fujiwara, K. Hara, K. Hatanaka, M. Itoh, Y. Kanada-En'yo, S. Kishi, K. Nakanishi, H. Sakaguchi, Y. Shimbara, A. Tamii, S. Terashima, M. Uchida, T. Wakasa, Y. Yasuda, H. Yoshida, and M. Yosoi, *Physics Letters B* **646**, 6 (2007).
- [39] Y. Kanada-En'yo, *Physical Review C - Nuclear Physics* **75**, 024302 (2007).
- [40] T. Yamada, Y. Funaki, H. Horiuchi, K. Ikeda, and A. Tohsaki, *Progress of Theoretical Physics* **120**, 1139 (2008).
- [41] Y. Chiba, M. Kimura, and Y. Taniguchi, *Physical Review C* **93**, 034319 (2016).
- [42] Y. Funaki, T. Yamada, H. Horiuchi, G. Röpke, P. Schuck, and A. Tohsaki, *Physical Review Letters* **101**, 082502 (2008).
- [43] M. Ito, *Physical Review C - Nuclear Physics* **83**, 044319 (2011).
- [44] T. Yamada, Y. Funaki, T. Myo, H. Horiuchi, K. Ikeda, G. Röpke, P. Schuck, and A. Tohsaki, *Physical Review C - Nuclear Physics* **85**, 034315 (2012).
- [45] T. Ichikawa, N. Itagaki, Y. Kanada-En'Yo, T. Kokalova, and W. Von Oertzen, *Physical Review C - Nuclear Physics* **86**, 031303 (2012).
- [46] Z. H. Yang, Y. L. Ye, Z. H. Li, J. L. Lou, J. S. Wang, D. X. Jiang, Y. C. Ge, Q. T. Li, H. Hua, X. Q. Li, F. R. Xu, J. C. Pei, R. Qiao, H. B. You, H. Wang, Z. Y. Tian, K. A. Li, Y. L. Sun, H. N. Liu, J. Chen, J. Wu, J. Li, W. Jiang, C. Wen, B. Yang, Y. Y. Yang, P. Ma, J. B. Ma, S. L. Jin, J. L. Han, and J. Lee, *Physical Review Letters* **112**, 162501 (2014).
- [47] Y. Kanada-En'Yo, *Physical Review C* **89**, 024302 (2014).

- [48] T. Yamada and Y. Funaki, *Physical Review C* **92**, 034326 (2015).
- [49] Y. Chiba and M. Kimura, *Physical Review C* **91**, 061302 (2015).
- [50] Y. Chiba, Y. Taniguchi, and M. Kimura, *Physical Review C* **95**, 044328 (2017), arXiv:1610.04000.
- [51] M. Nakao, H. Umehara, S. Ebata, and M. Ito, *Physical Review C* **98**, 054318 (2018).
- [52] Y. Kanada-En'yo and Y. Shikata, *Physical Review C* **100**, 014301 (2019).
- [53] Y. Chiba and M. Kimura, *Physical Review C* **101**, 024317 (2020).
- [54] Y. Kanada-En'yo and K. Ogata, *Physical Review C* **101**, 014317 (2020).
- [55] T. Baba and M. Kimura, (2020), arXiv:2005.03934.
- [56] M. Itoh, S. Kishi, H. Sakaguchi, H. Akimune, M. Fujiwara, U. Garg, K. Hara, H. Hashimoto, J. Hoffman, T. Kawabata, K. Kawase, T. Murakami, K. Nakanishi, B. K. Nayak, S. Terashima, M. Uchida, Y. Yasuda, and M. Yosoi, *Physical Review C - Nuclear Physics* **88**, 064313 (2013).
- [57] Y. Kanada-En'yo, M. Kimura, and H. Horiuchi, *Comptes Rendus Physique* **4**, 497 (2003).
- [58] Y. Kanada-En'yo, M. Kimura, and A. Ono, *Progress of Theoretical and Experimental Physics* **2012**, 1A202 (2012).
- [59] M. Kimura, T. Suhara, and Y. Kanada-En'yo, *The European Physical Journal A* **52**, 373 (2016).
- [60] Y. Kanada-En'yo and M. Kimura, *Physical Review C - Nuclear Physics* **72**, 064322 (2005).
- [61] M. Kimura and H. Horiuchi, *Nuclear Physics A* **767** (2006), 10.1016/j.nuclphysa.2005.12.006.
- [62] Y. Taniguchi, M. Kimura, Y. Kanada-En'yo, and H. Horiuchi, *Physical Review C - Nuclear Physics* **76**, 044317 (2007).
- [63] Y. Taniguchi, Y. Kanada-En'yo, and M. Kimura, *Physical Review C - Nuclear Physics* **80**, 044316 (2009).
- [64] Y. Taniguchi and M. Kimura, *Physics Letters, Section B: Nuclear, Elementary Particle and High-Energy Physics* **800** (2020), 10.1016/j.physletb.2019.135086.
- [65] J. Berger, M. Girod, and D. Gogny, *Computer Physics Communications* **63**, 365 (1991).
- [66] M. Kimura, *Physical Review C* **69**, 044319 (2004).
- [67] Y. Taniguchi, M. Kimura, and H. Horiuchi, *Progress of Theoretical Physics* **112**, 475 (2004).
- [68] D. L. Hill and J. A. Wheeler, *Physical Review* **89**, 1102 (1953).
- [69] Y. Chiba and M. Kimura, *Progress of Theoretical and Experimental Physics* **2017** (2017), 10.1093/ptep/ptx063.

- [70] H. Horiuchi, *Progress of Theoretical Physics* **47**, 1058 (1972).
- [71] H. Horiuchi, *Progress of Theoretical Physics Supplement* **62**, 90 (1977).
- [72] R. R. Rodríguez-Guzmán, J. L. Egido, and L. M. Robledo, *Physical Review C - Nuclear Physics* **62**, 543081 (2000).
- [73] T. Inakura, S. Mizutori, M. Yamagami, and K. Matsuyanagi, *Nuclear Physics A* **710**, 261 (2002).
- [74] M. Bender, H. Flocard, and P. H. Heenen, *Physical Review C - Nuclear Physics* **68**, 13 (2003).
- [75] N. Curtis, A. S. J. Murphy, N. M. Clarke, M. Freer, B. R. Fulton, S. J. Hall, M. J. Leddy, J. S. Pople, G. Tungate, R. P. Ward, W. N. Catford, G. J. Gyapong, S. M. Singer, S. P. G. Chappell, S. P. Fox, C. D. Jones, D. L. Watson, W. D. M. Rae, P. M. Simmons, and P. H. Regan, *Physical Review C* **53**, 1804 (1996).
- [76] T. A. Carey, P. G. Roos, N. S. Chant, A. Nadasen, and H. L. Chen, *Physical Review C* **29**, 1273 (1984).
- [77] P. G. Roos, N. S. Chant, A. A. Cowley, D. A. Goldberg, H. D. Holmgren, and R. Woody, *Physical Review C* **15**, 69 (1977).
- [78] T. Yoshimura, A. Okihana, R. E. Warner, N. S. Chant, P. G. Roos, C. Samanta, S. Kakigi, N. Koori, M. Fujiwara, N. Matsuoka, K. Tamura, E. Kubo, and K. Ushiro, *Nuclear Physics A* **641**, 3 (1998).
- [79] K. Yoshida, K. Minomo, and K. Ogata, *Physical Review C* **94**, 044604 (2016).
- [80] K. Yoshida, K. Ogata, and Y. Kanada-En'Yo, *Physical Review C* **98**, 024614 (2018).
- [81] K. Yoshida, Y. Chiba, M. Kimura, Y. Taniguchi, Y. Kanada-En'Yo, and K. Ogata, *Physical Review C* **100**, 044601 (2019).
- [82] A. S. Reiner, *Nuclear Physics* **27**, 115 (1961).
- [83] C. Ouellet and B. Singh, *Nuclear Data Sheets* **112**, 2199 (2011).
- [84] R. B. Leachman, P. Fessenden, and W. R. Gibbs, *Physical Review C* **6**, 1240 (1972).
- [85] A. W. Obst and K. W. Kemper, *Physical Review C* **6**, 1705 (1972).